Publication V

A. La Magna, V. Privitera, Guglielmo Fortunato, Massimo Cuscunà, B. G. Svensson, E. Monakhov, K. Kuitunen, J. Slotte, and F. Tuomisto. 2007. Vacancy generation in liquid phase epitaxy of Si. Physical Review B, volume 75, number 23, 235201, pages 1-6.

© 2007 American Physical Society (APS)

Reprinted with permission from the American Physical Society.

Readers may view, browse, and/or download material for temporary copying purposes only, provided these uses are for noncommercial personal purposes. Except as provided by law, this material may not be further reproduced, distributed, transmitted, modified, adapted, performed, displayed, published, or sold in whole or part, without prior written permission from the American Physical Society.

http://link.aps.org/abstract/prb/v75/e235201

PHYSICAL REVIEW B **75**, 235201 (2007)

Vacancy generation in liquid phase epitaxy of Si

A. La Magna and V. Privitera
CNR-IMM Sezione Catania, Stradale Primosole 50, I-95121 Catania, Italy

Guglielmo Fortunato and Massimo Cuscunà
CNR-IFN, Via Cineto Romano 43, 00156 Roma, Italy

B. G. Svensson and E. Monakhov
Physical Electronics, Department of Physics, University of Olso, P.O. Box 1048, Blindern, N-0316 Oslo, Norway

K. Kuitunen, J. Slotte, and F. Tuomisto
Laboratory of Physics, Helsinki University of Technology, P.O. Box 1100 (Otakaari 1 M), FI-02015 TKK Espoo, Finland
(Received 17 November 2006; revised manuscript received 1 February 2007; published 6 June 2007)

Concerted experiments and theoretical analysis are applied to conclusively demonstrate the vacancy generation during fast melting and regrowth of Si by laser irradiation. Experiments, based on the positron annihilation spectroscopy and designed to test the theoretical predictions, evidence a vacancy supersaturation after the laser process depending on the irradiation conditions. Stochastic atomistic simulations of the molten Si recrystallization show trapping of vacancies in the recrystallized region. Finally, continuum phase-field simulations of the full process, calibrated using the Monte Carlo results, show a defect evolution in close agreement with the experiments.

DOI: 10.1103/PhysRevB.75.235201 PACS number(s): 61.72.Yx, 02.50.Ng, 42.62.−b, 68.35.Rh

I. INTRODUCTION

Point defect evolution in nonequilibrium conditions has attracted a broad interest in the past decades also due to the role played by the defects in the transient enhanced diffusion phenomena in Si. Such a huge research effort has produced a consistent scenario, elucidated by experimental and theoretical works, on the different stages (diffusion, aggregate nucleation, formation, and annihilation of extended defects) of defect supersaturation in Si at constant temperature. The defect kinetics in extremely far from equilibrium conditions (nonuniform fast varying thermal field and phase transition), like those caused by a laser irradiation (LI) process in the melting regime, has been instead poorly investigated. Indeed, while the phase-transition kinetics, including the concurrent impurity segregation and redistribution, has been quite extensively investigated both experimentally and theoretically,[1–4] the basic understanding of the microstructural modification caused by the laser irradiation of Si has not been fully achieved yet.

Currently, there is no clear consensus whether an excess of point defects emerges after LI of Si. A possible indirect evidence of a vacancy (V) supersaturation was reported in Ref. 5, where some anomalies of the depth distribution of B implanted in Si after LI were explained by assuming an accumulation of V's at the melt depth. Moreover, a V-type residual damage[6] has been invoked in order to explain the reduction of the boron transient enhanced diffusivity, occurring in thermally treated B implanted Si samples after being irradiated by laser. Nevertheless, no direct measurement has been carried out so far and, particularly, no quantification of these phenomena has been made. The aim of this work is predicting quantitatively the V-type defect distribution emerging after the ultrarapid liquid-solid interface motion, occurring for melting LI. In Sec. II, we discuss the performed experiments in order to evidence the V-type defect formation in a controlled setting. Positron annihilation measurements are applied to characterize the dependence on the irradiation conditions (pulse energy and number of shots) of the residual damage after a multishot LI process. We present in Sec. III the stochastic method we have used to investigate at the atomic level the defect generation during the recrystallization of Si. The dependence of the V generation efficiency on undercooling is the fundamental result obtained by means of these investigations.

The knowledge of this dependence allows us to implement a continuum model, discussed in Sec. IV, aimed to simulate the damage evolution during a full multishot LI (i.e., during the pulse duration and in the time interval between two pulses) in order to compare directly the simulations with the positron annihilation measurements. Both experimental and theoretical results are discussed and commented in Sec. V.

II. EXPERIMENT

We have investigated experimentally the microstructural modification occurring in laser-irradiated Si samples by positron annihilation spectroscopy (PAS). A Lambda Physik LPX 205 XeCl excimer laser ($\lambda=308$ nm, 28 ns pulse duration, and 6×6 mm^2 spot) in the multishot (1–100) regime was used for the experiments. The samples were cut from n-type Czochralski (Cz) wafers with a resistivity of $\sim1\ \Omega$ cm. LI was performed in vacuum, at RT and fluences of 1.0 and 1.2 J/cm^2. Positron annihilation spectroscopy is sensitive to defects containing an open volume. We used a low-energy positron beam with Ge detectors to measure the Doppler broadened energy spectrum of the annihilation radiation. The shape of the peak was described using the conventional shape parameter S, which describes the positron annihilation fraction with low momentum (valence) elec-

 ©2007 The American Physical Society

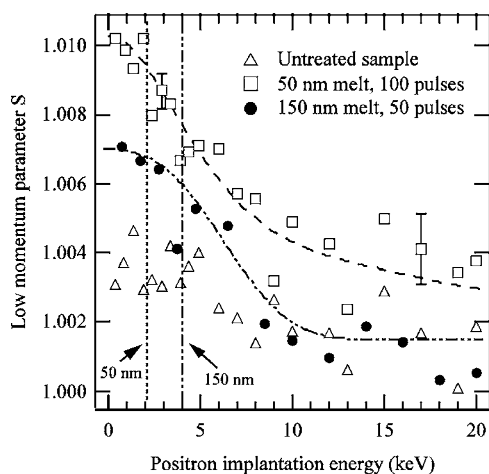

FIG. 1. The low momentum S parameter as a function of positron implantation energy in the untreated sample and samples after annealings with 100 and 50 laser pulses with 50 and 150 nm melts, respectively. The dotted curves are drawn to guide the eyes.

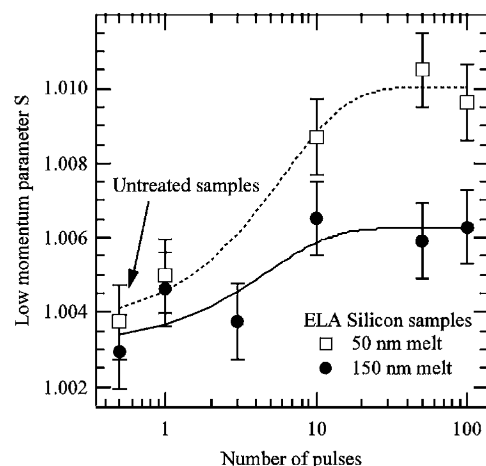

FIG. 2. The low momentum S parameter as a function of the number of the laser annealing pulses. The solid and dashed curves are drawn to guide the eyes.

trons. The increase of the S parameter above the bulk value is the signature of V-type defects being present in the material. The measurements were carried out at room temperature, where the lower detection limit for the vacancy concentration is $\sim 10^{16}$ cm^{-3}. The native oxide on the surface of the samples distracts the positron data by lowering the S parameter in the vicinity of the surface (see Ref. 7). Therefore, prior to the measurements, all the samples were etched in HF to remove the native oxide. A thorough description of the measurement method can be found in Ref. 8.

The S parameter is shown in Fig. 1 as a function of the positron implantation energy in an untreated sample and in samples irradiated with 100 (1.0 J/cm^2) and 50 (1.2 J/cm^2) laser pulses ($\approx$50 and $\approx$150 nm melt depths, respectively). The parameters have been scaled to the values measured in the bulk (S_{bulk}=0.528). The increase of the S parameter in the near surface region is a clear evidence of V-type defects in the regrown layer. Indeed, the value of the S parameter in irradiated samples is definitively larger than its value in untreated samples. The effect is stronger in the sample with a 50 nm melted layer. Figure 2 shows how the S parameter (average values in the range 1–2 and 1–4 keV for the samples with 50 and 150 nm melt depths, as indicated by the dashed lines in Fig. 1) increases with the number of laser pulses in the near surface region until saturation is reached after $\approx$10 pulses. This indicates that the total observed open volume increases with the number of pulses. We note that, even though the evidence is clear, the exact identification of the vacancy defects is difficult due to the vicinity of the surface.

III. ATOMISTIC SIMULATION OF ULTRAFAST REGROWTH PHENOMENA

In order to support the PAS data with a quantitative theoretical analysis, we have developed a multiscale methodology, where the generation of V-type defects during the regrowth phenomena (lasting a few nanoseconds) is investigated by means of an atomistic stochastic approach while the evolution of the generated defects during the full multishot process (lasting for 100 s) is simulated by means of the continuum model, based on partial differential equations, described in Sec. IV.

We have applied a kinetic lattice Monte Carlo (KLMC) approach to simulate the recrystallization kinetics of a large system. KLMC is the reliable method to quantitatively investigate the defect generation. Indeed, while a single generation event can be studied by means of a more accurate approach (e.g., molecular dynamics[9]), KLMC allows large scale simulation and, therefore, the quantification of the dependence of the generation rate as a function of the interface speed V_{sl} or the undercooling (these two quantities are correlated[1]).

The Si diamond lattice is the reference lattice of the code; therefore, no interstitial-like configuration can be studied. This approximation is reliable when simulating the ultrafast regrowth phenomena induced by LI. Indeed, molecular-dynamics simulations[9] have shown that the regime of generation of vacancies at the liquid-solid interface, in terms of interface speed V_{sl}, is separated from the regime of formation of interstitials. There is a critical value of $(V_{sl}/G)_c \approx 0.1$ mm^2/min K (where G is the thermal gradient at the interface) above which vacancies form. We have evaluated that, in our irradiation conditions, the interface speed is very high [$V_{sl} > 2$ m/s (Ref. 1)] and the V_{sl}/G value is well above the $(V_{sl}/G)_c$ threshold during the solidification in our samples. In these conditions, the eventual generation of interstitials can be neglected.

KLMC simulates the regrowth of a partially molten Si system as a sequence of elementary atomic events occurring at the solid-liquid interface (i.e., no kinetics occurs in the bulk liquid or solid phase). Each site of the reference lattice is marked as liquid (L site) or solid (S site) in order to separate the two regions; however, the real atomic occupancy of lattice sites can be strictly considered only for the solid region (i.e., S sites are really Si atoms in the crystalline phase). The Monte Carlo events are the transitions of lattice sites at the solid-liquid interface (which, in this case, are the KLMC

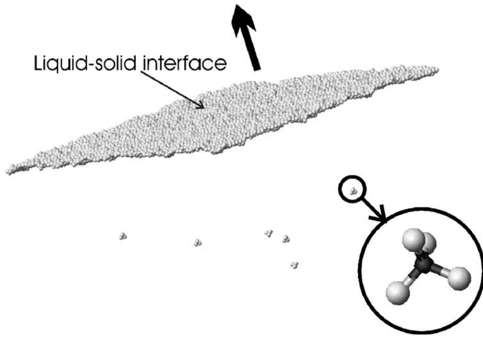

FIG. 3. Undercoordinated atoms in the solid region obtained after $t=2.613$ ns of evolution simulated by our KLMC code for a partially molten Si system at $T=1660$ K. The thick arrow indicates the regrowth direction. A zoom view of the undercoordinated atoms next neighbor of a vacancy trapped in the bulk region is also shown.

particles) which are promoted from the liquid phase to the solid one (i.e., an L site becomes S site) and vice versa. An L site is a vacancy site in the bulk solid region if all its next neighbors are S sites. If this condition occurs during the simulated evolution, the site cannot be promoted to the solid phase. The transition occurring at a given time of the simulated evolution is stochastically selected in the list of possible transitions (continuous time algorithm[10]) according to its own probability, assigned on the basis of the particle energetics. The transition probability of a solid to liquid event is[11]

$$P_{SL} = P_0 \exp[-n_S(\Phi_S - \Phi_L)/k_B T], \tag{1}$$

where n_S is the number of bonds which the interface site forms with atoms in the solid phase, Φ_S is the bond energy when the bond is formed by two atoms in the solid phase, and Φ_L is the bond energy when one of the two atoms forming the bond is in the liquid phase. Similarly, the transition probability of a liquid to solid event is

$$P_{LS} = P_0 \exp[-\Delta S/k_B], \tag{2}$$

where $\Delta S/k_B = 2(\Phi_S - \Phi_L)/k_B T_M$ is the entropy of fusion and $T_M = 1688$ K is the melting point of Si. The value of bond difference for Si used in the simulation is $\Phi_S - \Phi_L = 0.96$ eV,[12] while the probability prefactor P_0 is calibrated by correlating the simulated interface speed with the experimental interface speed $V_{sl}(T)$ as a function of temperature.[13] Note that, in our KLMC code, solidification events can occur at all sites at the solid-liquid interface which are next neighbor of a "solid atom." This feature makes our model slightly different with respect to conventional solid-on-solid models, which formally disallow vacancy formation in the bulk crystal.[12,14]

In Fig. 3, a snapshot of the undercoordinated atoms, obtained after $t=2.613$ ns of simulated evolution of an undercooled partially molten Si system ($T=1660$ K), is shown. The dimension of the simulation box is $64 \times 64 \times 64\ a_{\mathrm{Si}}^3$, where $a_{\mathrm{Si}} = 0.543$ nm is the Si lattice conventional unitary cell. Semiperiodical boundary conditions are imposed (i.e., the system is periodic along the x-y plane) and the initial liquid-solid (100) interface is set at the position $z_{in} = 8a_{\mathrm{Si}}$

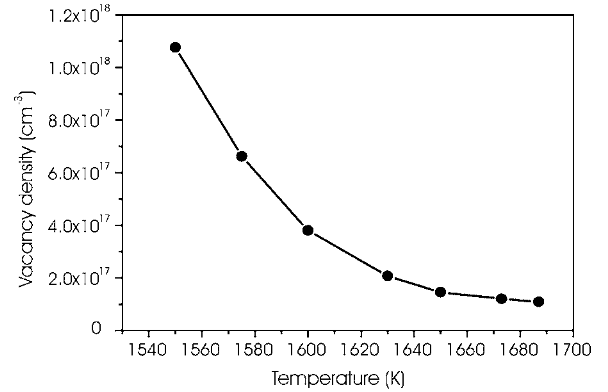

FIG. 4. Density of the vacancy-type defects generated in the simulated solidification process as function of the temperature.

along the (001) direction, which, in our representation, coincides with the z axis. Therefore, the initial system is liquid in the $z > z_{in}$ region and solid in the $z < z_{in}$ region.

The simulated system undergoes a solidification if an undercooling $T < T_M$ is imposed. At the time of the snapshot reported in Fig. 3, the regrown layer is ~6.7 nm thick [$V_{sl}(T=1660\ \mathrm{K}) \cong 2.6$ m/s]. The liquid-solid interface is rough at the atomic scale, as we should expect since it moves along the (001) direction. The KLMC model predicts the formation of vacancy-type intrinsic defects as a consequence of the solidification process. Indeed, the threefold coordinated atoms in the bulk solid region correspond to the nearest-neighbor atoms of lattice sites occupied by vacancies (four threefold coordinated atoms for each vacancy).

We have studied the vacancy formation as a function of undercooling using larger ($128 \times 128 \times 128\ a_{\mathrm{Si}}^3$) simulation boxes containing 16 777 126 sites. Also, for this analysis, we use semiperiodical boundary conditions, while the initial liquid-solid (100) interface is set at the position $z_{in} = 16a_{\mathrm{Si}}$ along the (001) direction. In Fig. 4, the average vacancy density $C_V^*(T)$ calculated in the whole simulation box is shown as a function of undercooling temperature [we could also correlate C_V^* to the interface speed using the $V_{sl}(T)$ relationship]. In each simulation, $C_V^*(T)$ is evaluated as an average value of the vacancy density in an ~52 nm thick regrown layer. Moreover, in order to improve the accuracy of the estimate, the $C_V^*(T)$ values derived in ten replicas of the KLMC evolution have been statistically analyzed.

The total amount of generated defects increases with undercooling, whereas it saturates at a level of $\sim 10^{17}$ cm^{-3} when the undercooling tends to zero. We note that, when the undercooling is low, the reliability of the KLMC simulations, which do not consider I-type defect generation, is questionable. Indeed, in the near-equilibrium growth (e.g., in the case of a bulk-crystal-grown Cz process of Si), both V-type and I-type defects could form. Therefore, the 10^{17} cm^{-3} concentration, predicted by the KLMC simulations in the limit of zero undercooling, could be related to the net vacancy density trapped in "localized region" (where G is known to be very low and therefore $V_{sl}/G > 0.1$ mm^2/min) of the Si Cz grown ingots. We point out that, in our irradiation conditions (very large V_{sl}), pure V generation occurs. The increase of the defect trapping efficiency with undercooling is strictly

related to moving away from equilibrium conditions, which causes also an increase of the interface speed. Indeed, at the atomic level, the interface net motion is due to the imbalance between the liquid-to-solid transitions with respect to the solid-to-liquid ones, which obviously increases with undercooling. As a consequence, when the undercooling increases, it is less and less probable that a defect, formed by fluctuation at the solid side of the solid-liquid interface after a liquid-to-solid transition, is dynamically annihilated by the back solid-to-liquid transition.

IV. VACANCY-TYPE DEFECT EVOLUTION IN A MULTISHOT LASER PROCESS

In order to conclusively determine the depth distribution of the V-type defects arising from multishots irradiation processes, as those performed in our experiments, we have developed a kinetic phase-field model calibrated by means of the KMLC results. Indeed, while the generation occurs during the very fast regrowth phenomena lasting $\sim$100 ns and can be theoretically investigated by means of KLMC simulation, the PAS measurements have been performed after 100 cycles of irradiation and subsequent cooling down, i.e., in this case after 100 s, that is outside the range of application of the KLMC approach. During cooling down, the vacancies diffuse and form aggregates due to encounter events, and they can also recombine with the interstitials present at the thermal equilibrium in the bulk; therefore, clustering and recombination events must be considered in the modeling.

The phase-field methodology is based on a physical description of the moving phase boundary problem, considering a finite dimension of the transition region between the two phases.[1] In order to describe the V-type defect evolution by means of this numerical technique, we need to include, as presented in the following, the generation level $C_V^*(T)$ derived by KLMC in the continuum model. In the numerical simulations, phase Φ ($0 \leqslant \Phi \leqslant 1$, with $\Phi=1$ and $\Phi=0$ for the pure solid and liquid phases, respectively) and temperature T evolve concurrently ruled by the following coupled differential equations:

$$\dot{\Phi} = D_\Phi \nabla^2 \Phi - D_\Phi / l^2 \{\Phi[1-\Phi][0.5+\beta(T)-\Phi]\}, \quad (3)$$

$$\rho c_V \dot{T} + 6\Phi(1-\Phi) L_{\mathrm{Si}} \dot{\Phi} = \nabla K(\Phi) \nabla T + S(\mathbf{r},t). \quad (4)$$

In these equations, l is the interface thickness, L_{Si} the latent heat of pure silicon, ρ the Si density, c_V the (constant volume) specific heat, D_Φ the phase-field diffusivity, and $K(\Phi)$ the phase dependent thermal conductivity. $\beta(T)$ depends on the interface speed by means of the relation $\beta(T) = lV_{sl}(T)/2D_\Phi$. We indicate with $S(\mathbf{r},t)$ the time- and space-dependent external heat source due to irradiation, which can be derived from the known dependence of the laser-pulse power density as a function of time. We do not report here the phase-field parameter calibration, since a detailed discussion concerning the calibration and the list of used values of these parameters can be found in Ref. 1.

The vacancy generation at the moving interface, the vacancy clustering phenomena, and the overall V supersaturation kinetics during cooling down can be considered by coupling Eqs. (3) and (4) with the following equations for the vacancy C_V and divacancy (V_2) C_{2V} density evolution:

$$\dot{C}_V = \nabla D_V(T) \nabla C_V - C_V^*(T) 6\Phi(1-\Phi)\dot{\Phi} - 2R_{V,V} - R_{V,I} + R_{V_2,I} \quad \text{if } \Phi \neq 0, \quad (5)$$

$$\dot{C}_{V_2} = \nabla D_{V_2}(T) \nabla C_{V_2} + R_{V,V} - R_{V_2,I} \quad \text{if } \Phi \neq 0, \quad (6)$$

where the reaction-type terms are

$$R_{I,V} = 4\pi(D_I + D_V) a_{\mathrm{Si}} \exp(-E_{I,V}^{forw}/kT)[C_I C_V - \{C_I\}^* \{C_V\}^*],$$

$$R_{V,V} = 8\pi D_V a_{\mathrm{Si}} \exp(-E_{V,V}^{forw}/kT)[C_V C_V - K_{V,V}^{back}(T) C_{V_2}],$$

$$R_{V_2,I} = 4\pi(D_{V_2} + D_I) a_{\mathrm{Si}} \exp(-E_{V_2,I}^{forw}/kT)[C_{2V} C_I - C_V \{C_{V_2}\}^* \{C_I\}^* / \{C_V\}^*],$$

with the condition $C_V \equiv 0$, $C_{V_2} \equiv 0$ if $\Phi = 0$, which states the complete vacancy-type defect annihilation in the liquid phase. We note that the link between KLMC and phase-field simulation is the second phase dependent term in the right-hand side of Eq. (5). This term allows vacancy generation at a level $C_V^*(T)$ at the moving boundary, which depends on the temperature field at the solid-liquid interface, and it is consistently evaluated by the continuum model [see Eq. (3)]. Of course, $C_V^*(T)$ is set using the curve shown in Fig. 4.

We have considered the divacancy clusters as representative of the residual damage emerging after the process, even if we cannot exclude the formation of larger vacancy clusters or other trapping configuration. However, since no Ostwald-ripening-type phenomenon can occur in the ultrafast quenching, following the laser pulse, the formation of larger V-type clusters is a higher-order process due to the encounter between a free V and a previously formed V_2. Hence, we assume that the simulated C_{V_2} profile is a reliable approximation of the residual V-type defect profile measured by positron annihilation.

In Eq. (5), C_I is the interstitial density, $D_V(T)$ and $D_{V_2}(T)$ are the T-dependent vacancy and divacancy diffusivities. The continuum model includes the divacancy formation term $R_{V,V}$, and bulk recombination terms with I, $R_{V,I}$, $R_{V_2,I}$. Diffusion-limited coefficients for forward reactions are assumed, while the back reactions in the recombination term are driven by the equilibrium, and an Arrhenius-type relation for the back reaction in the divacancy formation term is considered,

$$K_{V,V}^{back}(T) = \rho_{\mathrm{Si}} \exp(-E_{V_2}^{bind}/k_B T),$$

where $\rho_{\mathrm{Si}} = 5.0 \times 10^{22}$ cm^{-3} is the silicon atomic density and $E_{V_2}^{bind}$ the divacancy binding energy. In the simulations, we use the theoretical estimate of Ref. 15 for the calibration of the parameters of free point defects, $\{C_I\}^* = \rho_{\mathrm{Si}} \exp(11.2)\exp(-3.7 \text{ eV}/kT)$ and $\{C_V\}^* = \rho_{\mathrm{Si}} \exp(9)\exp$

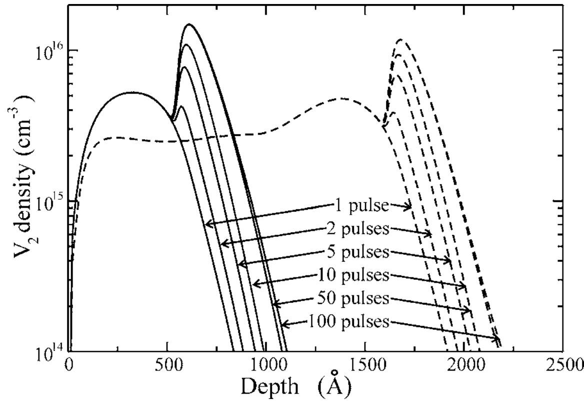

FIG. 5. Divacancy density profiles obtained by means of phase-field simulated evolution of a 100 pulse irradiation process at 1.0 J/cm^2 (solid lines) and 1.2 (dashed lines) fluences. Profiles obtained after 1, 2, 5, 10, 50, and 100 pulses are shown.

$(-3.97\ \mathrm{eV}/kT)$ cm^{-3}; $D_I=0.158\exp(-1.37\ \mathrm{eV}/kT)$ and $D_V=(1.18\times10^{-4})\exp(-0.1\ \mathrm{eV}/kT)$ cm^2/s; $E^{forw}_{I,V}=E^{forw}_{V_2,I}=0$. Since only vacancy supersaturation $C_V>\{C_V\}^*$ is caused by the irradiation, we do not include in the model the diffusion equation for the interstitial and we set $C_I(T)\equiv\{C_I(T)\}^*$ (as we should expect in the absence of I supersaturation) in the quenching interval between two subsequent pulses.

By using the phase-field model, we have simulated the experimental irradiation processes; then, we have considered 100 pulse irradiation ($\lambda=308$ nm, ~28 ns pulse duration) of a (100) oriented c-Si at 1.0 and 1.2 J/cm^2 fluences at room temperature. The system evolution during each pulse is followed after the complete resolidification until the thermal field quenches back to room temperature in the whole sample. The divacancy profiles, obtained by means of the simulation after each pulse, relative to the 1.0 and 1.2 J/cm^2 cases, are shown in Fig. 5 for the divacancy related parameters suggested in Ref. 16 ($D_{V_2}=(3\times10^{-3})\exp[-1.3\ \mathrm{eV}/kT]$, $E^{bind}_{V_2}=1.7$ eV, and $E^{forw}_{V,V}=0.3$ eV). The defects generated by the regrowth process evolve in the solid phase due to the fast varying high-temperature field induced by the irradiation. We follow the evolution after quenching to RT for the time interval (1 s) between two pulses. We have verified that after this time, the free vacancies completely recombine with I and at the surface. The subsequent laser pulse annihilates the residual vacancy clusters residing within the melt depth ($\approx$50 nm for the 1.0 J/cm^2 case and $\approx$150 nm for the 1.2 J/cm^2 case), but the divacancy profiles extend well beyond the melt depth due to the fast diffusion of vacancies, and hence the subsequent melting shot does not remove all the defects generated by the previous pulse. As a consequence, V-type clusters accumulate, pulse by pulse, near the region affected by melting and regrowth, reaching a peak density above 10^{16} cm^{-3}. We have performed different simulations modifying the model calibration, i.e., changing the point defect related parameters (e.g., using the values suggested in Ref. 17) and the V_2 formation barrier $E^{forw}_{V,V}$. The features of the simulated damage redistribution (accumulation and saturation at large number of pulses) are essentially similar when the setting is modified; however, the total amount of the residual damage could change (e.g., the peak density varies in the 10^{16}–10^{17} cm^{-3} range).

V. DISCUSSION AND CONCLUSION

The accumulation of V-type defects simulated by means of our theoretical approach consistently confirms the positron annihilation measurements that detect vacancy-type defects in the proximity of a liquid phase epitaxially regrown layer. Experimental analysis and phase-field simulations show a similar scenario for the evolution of the V-type defects in laser-irradiated Si in a multishot configuration. The defects accumulate over subsequent pulses, and a saturation of the material modification is observed for large number of pulses. We note that, since the phase-field simulations are calibrated by using the generation level $C^*_V(T)$ derived by KLMC, the continuum approach correlates directly the experimental data with the atomistic simulation results. The positron implantation profile broadens with increasing implantation energy,[7] yielding a poorer depth resolution and smearing out well-confined peaks. Hence, the weaker effect in the samples with 150 nm melt could be caused either by a lower total concentration of vacancy defects in the melted layer or by a peaked concentration profile located at the maximum melt depth, as predicted by the calculations. Based on the ~1% increase of the S parameter in the laser annealed samples, we estimate the vacancy defect concentration to be in the 10^{16} cm^{-3} range in the melted layers, as predicted by the simulation.

It is interesting to compare the effect of the same irradiation process for different sample preparation conditions. Indeed, a LI in the melting configuration can cause an opposite effect when the irradiation is performed after implantation.[18] In implanted samples, a huge density of Frenkel I-V pairs is present before the irradiation; hence, the result of subsequent irradiation is the trade-off between the generation at the moving interface and the annihilation (due to the melting) of the defects, generated by the implantation. Therefore, when a V-type supersaturation due to ion implantation arises, as in the case of Sb implants in Si,[18] the LI can provoke a decrease of such supersaturation, since it annihilates preferentially the V-type component of the Frenkel pairs, residing nearer the surface, with respect to the I-type component. Of course, such consideration does not apply in our experimental case since we perform irradiation in virgin samples.

Summarizing, in this work we have studied the microstructural modification due to LI of Si samples. The generation of vacancies at the moving solid-liquid interface during solidification has been described by means of KLMC calculations and confirmed by positron annihilation measurements and phase-field simulations, both showing in close agreement an accumulation of V-type defects at the melt depth. These findings are quantitative contributions to the understanding of defect kinetics in extremely far from equilibrium conditions.

Interesting future extensions of our concerted numerical and experimental investigations might address the defect generation during LI in compound semiconductors, such as GaAs and GaP. However, the KLMC approach for these materials has to be generalized in order to include the possibility of simulating two atomic species with the relative energetics. This generalization could also allow us to observe the possible generation of two kinds of vacancies (one for each atomic species forming the compound), which could lead to the evidence of other complex features with respect to the case of elemental semiconductors such as Si.

ACKNOWLEDGMENTS

The authors acknowledge E. Rimini for useful discussions. This work was partially funded by the Italian Ministry of Research (MIUR) through the project PLAST_ICs (DM 17767) and by the University of Oslo/SMN.

[1] A. La Magna, P. Alippi, V. Privitera, G. Fortunato, M. Camalleri, and B. G. Svensson, J. Appl. Phys. **95**, 4806 (2004).

[2] A. La Magna, P. Alippi, V. Privitera, S. Scalese, S. Pannitteri, G. Fortunato, and M. Camalleri, Appl. Phys. Lett. **84**, 4738 (2004).

[3] S. Whelan, A. La Magna, V. Privitera, G. Mannino, M. Italia, C. Bongiorno, G. Fortunato, and L. Mariucci, Phys. Rev. B **67**, 075201 (2003).

[4] K. K. Ong, K. L. Pey, P. S. Lee, A. T. S. Wee, Y. F. Chong, K. L. Yeo, and X. C. Wang, Mater. Sci. Eng., B **114**, 25 (2004).

[5] G. Mannino, V. Privitera, A. La Magna, E. Rimini, E. Napolitani, G. Fortunato, and G. Mariucci, Appl. Phys. Lett. **86**, 051909 (2005).

[6] E. Monakhov, B. G. Svensson, M. K. Linnarsson, A. La Magna, M. Italia, V. Privitera, G. Fortunato, M. Cuscunà, and L. Mariucci, Appl. Phys. Lett. **87**, 192109 (2005).

[7] M. Rummukainen, I. Makkonen, V. Ranki, M. J. Puska, K. Saarinen, and H.-J. L. Gossmann, Phys. Rev. Lett. **94**, 165501 (2005).

[8] K. Saarinen, P. Hautojärvi, and C. Corbel, in *Identification of Defects in Semiconductors*, edited by M. Stavola (Academic, New York, 1998), p. 209.

[9] T. Motooka, K. Nishihira, R. Oshima, H. Nishizawa, and F. Hori, Phys. Rev. B **65**, 081304(R) (2002).

[10] A. La Magna and S. Coffa, Comput. Mater. Sci. **17**, 21 (2000).

[11] K. A. Jackson, G. H. Gilmer, and D. E. Temkin, Phys. Rev. Lett. **75**, 2530 (1995).

[12] D. L. Woodraska and J. A. Jaszczak, Surf. Sci. **374**, 319 (1997). A different estimate of the bonding parameter should be guessed when the melting phenomenon occurs in an amorphous or implanted sample. As a consequence, the estimate of generated defect density can change in these cases.

[13] For the calibration, we can apply the accurate analytical Fulcher-Vogel-like relationship for $V_{sl}(T)$ fitted by means of experimental data [see S. R. Stiffler *et al.*, Acta Metall. Mater. **40**, 1617 (1992)].

[14] K. M. Beatty and K. A. Jackson, J. Cryst. Growth **211**, 13 (2000).

[15] M. Tang, L. Colombo, J. Zhu, and T. Diaz de la Rubia, Phys. Rev. B **55**, 14279 (1997).

[16] M. Mikelsen, E. V. Monakhov, G. Alfieri, B. S. Avset, and B. G. Svensson, Phys. Rev. B **72**, 195207 (2005).

[17] H. Bracht, J. F. Pedersen, N. Zangenberg, A. N. Larsen, E. E. Haller, G. Lulli, and M. Posselt, Phys. Rev. Lett. **91**, 245502 (2003).

[18] H. Shut, S. W. H. Eijt, C. D. Beling, K. Ho, and Y. Takamura, Mater. Sci. Eng., B **124-125**, 283 (2005).